Mirror energy difference and the structure of loosely bound proton-rich nuclei around $A = 20$

Cenxi Yuan,[1,2] Chong Qi,[3] Furong Xu,[2,*] Toshio Suzuki,[4,5] and Takaharu Otsuka[6,7,8]

[1] *Sino-French Institute of Nuclear Engineering and Technology, Sun Yat-Sen University, Zhuhai 519082, China*
[2] *State Key Laboratory of Nuclear Physics and Technology, School of Physics, Peking University, Beijing 100871, China*
[3] *Royal Institute of Technology, AlbaNova University center, SE-10691 Stockholm, Sweden*
[4] *Department of Physics, College of Humanities and Sciences, Nihon University, Sakurajosui 3, Setagaya-ku, Tokyo 156-8550, Japan*
[5] *National Astronomical Observatory of Japan, Mitaka, Tokyo 181-8588, Japan*
[6] *Department of Physics, University of Tokyo, Hongo, Bunkyo-ku, Tokyo 113-0033, Japan*
[7] *Center for Nuclear Study, University of Tokyo, Hongo, Bunkyo-ku, Tokyo 113-0033, Japan*
[8] *National Superconducting Cyclotron Laboratory, Michigan State University, East Lansing, Michigan, 48824, USA*

(Dated: April 22, 2014)

The properties of loosely bound proton-rich nuclei around $A = 20$ are investigated within the framework of nuclear shell model. In these nuclei, the strength of the effective interactions involving the loosely bound proton $s_{1/2}$ orbit are significantly reduced in comparison with those in their mirror nuclei. We evaluate the reduction of the effective interaction by calculating the monopole-based-universal interaction (V_{MU}) in the Woods-Saxon basis. The shell-model Hamiltonian in the *sd* shell, such as USD, can thus be modified to reproduce the binding energies and energy levels of the weakly bound proton-rich nuclei around $A = 20$. The effect of the reduction of the effective interaction on the structure and decay properties of these nuclei is also discussed.

PACS numbers: 21.10.Sf, 21.10.Dr, 27.30.+t, 21.60.Cs

arXiv:1404.5202v1 [nucl-th] 21 Apr 2014

I. INTRODUCTION

The study of proton-rich nuclei plays an important role in the understanding of a variety of nuclear astrophysical processes [1], such as the $^{17}\mathrm{F}(p,\gamma)^{18}\mathrm{Ne}$ reaction in stellar explosions [2]. The excitation spectra of proton-rich nuclei are similar to those in their mirror partners because the strong Nucleon-Nucleon (NN) interaction is almost charge independent and the influence of the Coulomb interaction on the excitation spectra is relatively small [3, 4].

For heavier nuclei in the *fp* shell, the energy difference between mirror states (MED) are rather small (usually only around 0.1 MeV) [5–7]. However, for light nuclei, the MED can be one order of magnitude larger. For example, the energy of the $1/2^+_1$ state in ^{13}N is 0.72 MeV lower than that in ^{13}C [8]. This shift in energy is related to the loosely bound nature of the proton $1s_{1/2}$ orbit [9, 10]. Since there is no centrifugal barrier, the radial wave function of the $1s_{1/2}$ orbital extends into a much larger space than those of other neighboring orbitals. Thus the Coulomb energy of the weakly bound $1s_{1/2}$ orbit, $\langle 1s_{1/2}|V_C|1s_{1/2}\rangle$, is less repulsive than those of other orbits and forms the shift of the $1/2^+_1$ state from ^{13}C to ^{13}N. Due to the Coulomb force and the isospin-nonconserving term of the nuclear force, the residual interaction V^{pp} in proton-rich nuclei are typically a few percent weaker than the corresponding V^{nn} in their mirror nuclei [11]. However, for the V^{pp} related to the weakly bound $1s_{1/2}$ orbit, the ratio V^{pp}/V^{nn} can be as small as 0.7, which can be deduced from observed data in nuclei around ^{16}O [12].

In nuclei around $A = 20$, where the $1s_{1/2}$ orbit plays an important role, the excitation energies of some states in proton-rich nuclei show large discrepancy when compared to their mirror states. For example, the astrophysically important 3^+_1 state in ^{18}Ne is lower than the corresponding state in ^{18}O by about 800 keV [2]. This 3^+_1 state in ^{18}Ne is above the proton separation threshold and quasi-bound due to the Coulomb barrier. It is expected that the following two aspects can be important in contributing to the difference between these mirror nuclei: the shift of the single particle energies and the reduction of the proton-proton residual interaction.

There are several well established shell-model Hamiltonians in the *sd* shell, such as USD [13], USDA [14] and USDB [14]. These are obtained by fitting to the binding energies and the excitation energies of the low-lying levels of nuclei with $N \geq Z$. However, proton-rich nuclei are affected by a mechanism not incorporated into the USD family even if they are phenomenologically optimized. The loosely binding effect of the proton orbitals is not taken into account in the USD family. On proton-rich side of the *sd* shell, the proton $d_{5/2}$ and $s_{1/2}$ orbitals are weakly bound or quasi bound in some nuclei, while both are deeply bound on the neutron-rich side.

In this paper, we will study the structure and decay properties of the weakly bound proton-rich nuclei around $A = 20$ by using the nuclear shell model with above effective interactions. It is expected that the binding energies and excitation spectra of these proton-rich nuclei can be

* frxu@pku.edu.cn

reproduced by modifying the single-particle energies and the two-body matrix elements (TBME) of the existing Hamiltonians. The weakly bound effect is dominated by the interplay between the spreading of radial wave functions and finite range properties of nuclear forces. Thus, the reduction factors of TBME are evaluated with the newly introduced NN interaction, monopole based universal interaction (V_{MU}) which has explicit dependence on the inter-nucleon distance and has been shown to be reasonable for basic properties like monopoles [15].

In this work we will evaluate the reduction effect of the TBME from a phenomenological point of view. It should be mentioned that the present work can also be helpful for future microscopic studies with realistic NN interaction. In particular, in Ref. [16], it is argued that the core-polarization effect can be dramatically suppressed in halo nuclei.

In Sec. II, we evaluate the reduction factors for the related TBME. The properties of loosely bound proton-rich nuclei around $A = 20$ are discussed in Sec. III. This work is summarized in Sec. IV.

II. THEORETICAL FRAMEWORK

The radial wave function of the proton $1s_{1/2}$ orbit in loosely bound proton-rich nuclei extends into a larger coordinate space than that of the neutron $1s_{1/2}$ orbit in the corresponding mirror nuclei. As an illustration, in Fig. 1 we show the calculated radial wave functions of the valence $1s_{1/2}$ orbits in nuclei ^{17}F and ^{17}O. The calculations are done with the Woods-Saxon potential with the depth $V_0 = 50.9$ (50.2) MeV for ^{17}F (^{17}O). The depths are determined by fitting to the single-particle energies of the $1s_{1/2}$ states, which are -0.10 MeV and -3.27 MeV in ^{17}F and ^{17}O, respectively [8]. Here, we assume that these energies can be set equal to measured one nucleon separation energies. These depths are close to the one given in Ref. [3]. The diffuseness and radius parameters in the Woods-Saxon potential are chosen to be $a = 0.67$ fm and $R = 1.27A^{1/3}$ fm [17], respectively, where A is the mass number of the nucleus. It can be clearly seen from Fig. 1 that the $1s_{1/2}$ orbit in ^{17}F has a larger space distribution than that in ^{17}O. Earlier experimental [18] and theoretical [19] analyses also show that the single proton in $1/2^+$ state in ^{17}F has very large space distribution. It should be mentioned that, for a reasonable set of Woods-Saxon parameters, the radial part of single-particle wave function is not sensitive to the detail of the potential. We find that the single-particle wave functions of the $0d_{5/2}$ orbit in ^{17}F and ^{17}O are rather similar to each other. The radial wave functions of the $0d_{3/2}$ orbital in ^{17}F and ^{17}O, both of which are unbound, are calculated using the code GAMOW [20] with above Woods-Saxon parameters. Despite the different outgoing waves because of the different resonant widths of the $3/2^+$ state in ^{17}F and ^{17}O, the radial wave functions of $0d_{3/2}$ orbit in these two nuclei are quite similar inside the nuclei. The $0d_{3/2}$ orbit is also

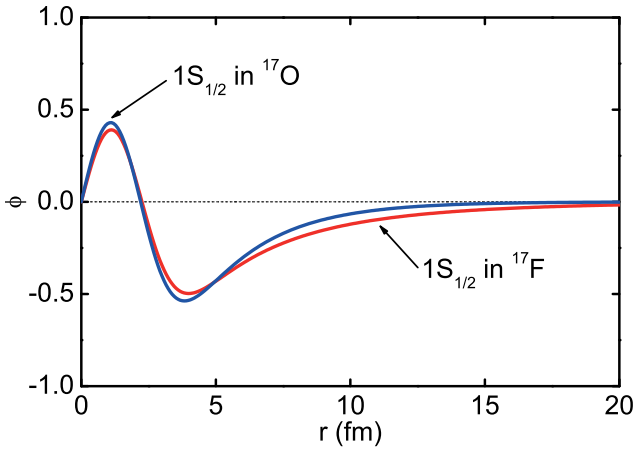

FIG. 1. (Color online) Single-particle wave functions of the $1s_{1/2}$ orbits in ^{17}O and ^{17}F.

relatively less important compared with $0d_{5/2}$ and $1s_{1/2}$ orbits in the study of low-lying states of the nuclei around $A = 20$. These are the reasons why only the TBME related to $1s_{1/2}$ proton need to be modified, which will be discussed later.

Our shell-model effective Hamiltonian is constructed starting from the well established USD, USDA and USDB interactions. The USD family has been determined by fitting to nuclei in the neutron-rich side by assuming isospin symmetry.

In the present work, the charge symmetry breaking of the NN interaction is not taken into account because the mirror differences are mostly caused by the weakly bound protons in the nuclei being studied as mentioned in the introduction. Calculations with the charge-dependent Bonn potential [7, 21] show that the effect of the charge dependence in the *sd* shell nuclei is rather minor. This is consistent with the result of Ref. [11]. The single-proton energy of the $1s_{1/2}$ orbit, relative to the one of the $0d_{5/2}$ orbit, of the shell-model Hamiltonian is lowered by 0.375 MeV as compared to the neutron one, by taking into account the fact that the experimental excitation energy of the $1/2^+_1$ state in ^{17}F is 0.375 MeV lower than that in ^{17}O.

The reduction factor of TBME, $f = \langle ij|V|kl\rangle^{pp}/\langle ij|V|kl\rangle^{nn}$, is obtained with the Woods-Saxon single-particle wave function and an effective NN interaction. Here we use V_{MU} [15] plus the spin-orbit force from the M3Y interaction [22] as the NN interaction. V_{MU}, which includes the Gaussian type central force and the $\pi + \rho$ bare tensor force, can explain the shell evolution in a large region of nuclei [15]. The original V_{MU} parameters can reproduce well the monopole part of SDPF-M and GXPF1A interactions in *sd* and *pf* regions [15]. The validity of the V_{MU} in shell-model calculation is examined in the *psd* [23] and *sdpf* [24, 25] regions. A similar method was used in Ref. [12] to evaluate the reduction factor by using the

TABLE I. Calculated reduction factors for the five proton-proton TBME in which the $1s_{1/2}$ orbit is involved.

TBME ($\langle ij\|V\|kl\rangle^{pp}_{JT}$)	Reduction factor
$\langle(1s_{1/2})^2\|V\|(1s_{1/2})^2\rangle^{pp}_{01}$	0.68
$\langle 1s_{1/2}0d_{5/2}\|V\|1s_{1/2}0d_{5/2}\rangle^{pp}_{31}$	0.78
$\langle 1s_{1/2}0d_{5/2}\|V\|1s_{1/2}0d_{5/2}\rangle^{pp}_{21}$	0.84
$\langle(0d_{5/2})^2\|V\|(1s_{1/2})^2\rangle^{pp}_{01}$	0.80
$\langle 1s_{1/2}0d_{5/2}\|V\|(0d_{5/2})^2\rangle^{pp}_{21}$	0.87

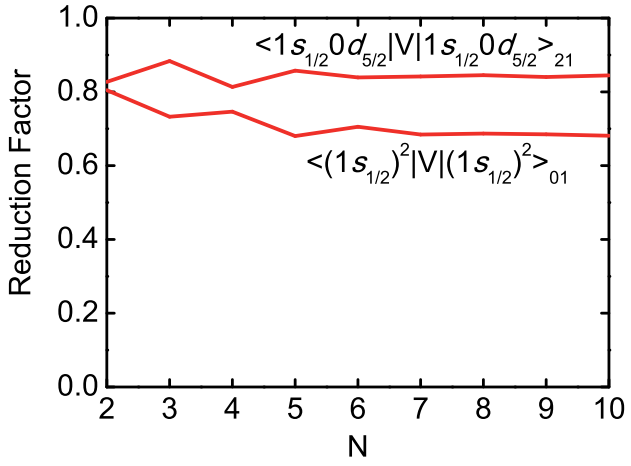

FIG. 2. (Color online) Reduction factors as the function of N, which means a Woods-Saxon wave function is expanded in N harmonic oscillator wave functions

M3Y interaction.

One needs a transformation from relative coordinate to usual shell-model coordinate in order to obtain TBME $\langle ij|V|kl\rangle$ from the NN interaction. We expand $\langle ij|V|kl\rangle_{WS}$ in harmonic oscillator basis. A Woods-Saxon single-particle wave function, e.g., $|1s_{1/2}\rangle_{WS}$, is expanded in ten harmonic oscillator single-particle wave functions, saying $|Ns_{1/2}\rangle_{HO}$ (N is from 0 to 9). The harmonic oscillator wave functions are calculated with the parameter $\hbar\omega = 45A^{-1/3} - 25A^{-2/3}$ ($A = 18$).

Our calculations thus show that only two-body interactions related to the proton $1s_{1/2}$ orbit are noticeably modified by calculations with the Woods-Saxon potential. In Table I we give the reduction factors of five proton-proton TBME involving the $1s_{1/2}$ orbit. A microscopic study shows a similar magnitude of reduction factors in weakly bound neutron-rich nuclei with Skyrme Hartree-Fock basis [26]. The reduction effect of other TBME is assumed to be much weaker, and is not taken into account in the following calculations for simplicity.

We have tested how the reduction factors depend on the mass number A and the number of harmonic oscillator shells N. The reduction factors are almost independent of A and converge after $N = 7$. Figure 2 gives the convergence of reduction factors for

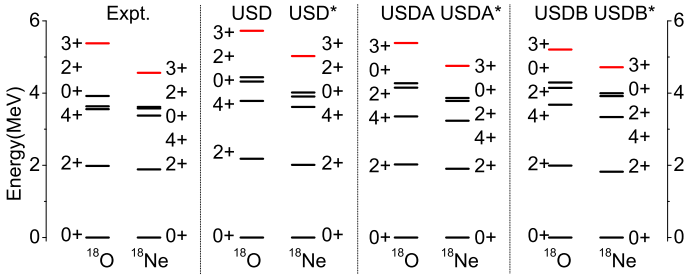

FIG. 3. (Color online) Experimental and calculated levels of the mirror nuclei ^{18}O and ^{18}Ne. USD*, USDA* and USDB* indicate the calculations with the modified proton-proton TBME (see Table I for exact modification factors and corresponding text for explanations). Data are from Ref. [8].

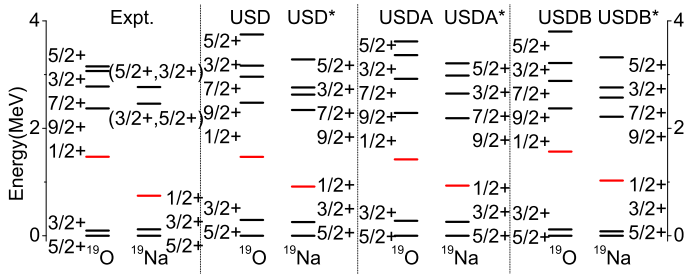

FIG. 4. (Color online) Same as Fig. 3 but for mirror nuclei ^{19}O and ^{19}Na. Data are from Refs. [8, 32, 33].

$\langle(1s_{1/2})^2|V|(1s_{1/2})^2\rangle^{pp}_{01}$ and $\langle 1s_{1/2}0d_{5/2}|V|1s_{1/2}0d_{5/2}\rangle^{pp}_{21}$ as the function of the numbers of harmonic oscillator basis which are used in our expansion of the Woods-Saxon wave function. Here, we evaluate the reduction factors through V_{MU} because the weakly bound effect of proton $1s_{1/2}$ orbit is not included in the USD family. As the USD family performs very well and is used widely in the study of neutron-rich side of the *sd* shell, we use the modified USD family to study the spectroscopic properties of the nuclei being studied. The Hamiltonians are labeled as USD*, USDA* and USDB* when the reduction modification is made.

III. THE STRUCTURE OF LOOSELY BOUND PROTON-RICH NUCLEI AROUND $A = 20$

Calculations are done in the *sd* shell by employing the shell model code OXBASH [27] with the effective Hamiltonians mentioned above. In the following, we will concentrate on proton drip-line nuclei ^{18}Ne, ^{19}Na, ^{20}Mg, $^{21-24}$Al and $^{22-24}$Si, where the proton $1s_{1/2}$ orbital is weakly or quasi bound. In Refs. [28–30], the proton-rich nuclei ^{18,19}Mg are studied within a Woods-Saxon potential model by considering the shell-model spectroscopic factors.

In Figs. 3 to 8 we show the comparison between the experimental and calculated energy levels of ^{18}Ne, ^{19}Na, $^{21-24}$Al and those of their mirror nuclei. The interac-

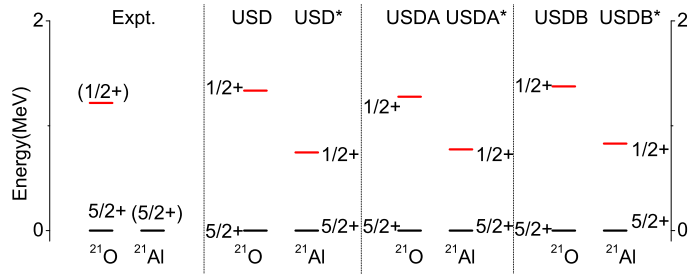

FIG. 5. (Color online) Same as Fig. 3 but for mirror nuclei ^{21}O and ^{21}Al. Data are from Ref. [8].

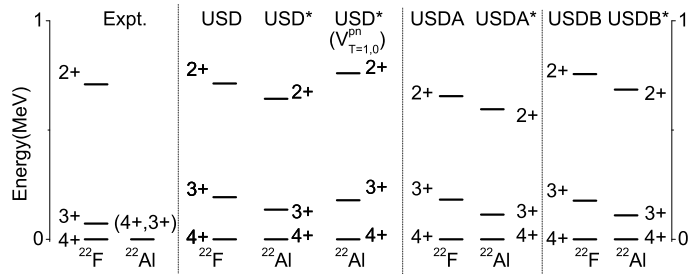

FIG. 6. (Color online) Same as Fig. 3 but for mirror nuclei ^{22}F and ^{22}Al. Data are from Ref. [8].

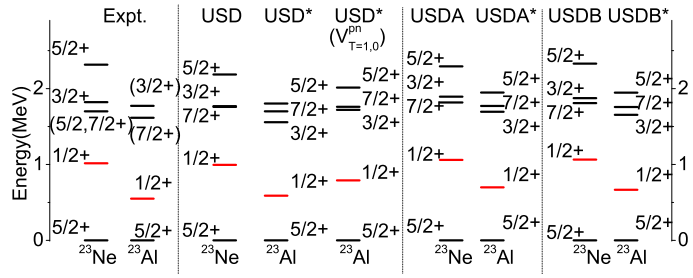

FIG. 7. (Color online) Same as Fig. 3 but for mirror nuclei ^{23}Ne and ^{23}Al. Data are from Refs. [8, 35].

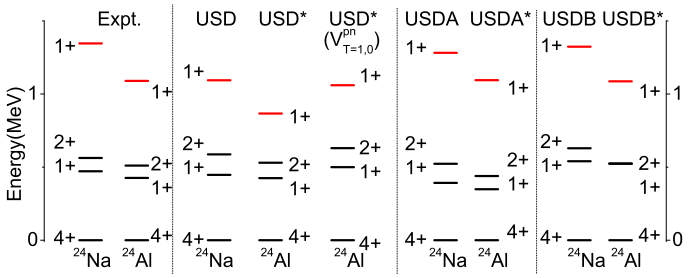

FIG. 8. (Color online) Same as Fig. 3 but for mirror nuclei ^{24}Na and ^{24}Al. Data are from Refs. [8, 37].

TABLE II. Experimental and calculated binding energies (in MeV) with the original and modified USD Hamiltonians. Data are from Ref. [38].

nucleus	Expt.	USD*	|Expt.−USD*|	USD	|Expt.−USD|
^{18}Ne	132.14	132.17	0.03	132.34	0.20
^{19}Na	131.82	131.85	0.03	131.95	0.13
^{20}Mg	134.48	134.81	0.33	134.97	0.49
^{21}Al		133.54		133.61	
^{22}Si		135.36		135.46	

tion, USD*($V^{pn}_{T=1,0}$), and related results in Figs. 6 to 8 will be discussed later. The original USD, USDA, USDB results can be found in Ref. [27]. It is thus seen that the MED's of the analogous states can be reproduced very well by the calculations. These results indicate MED's are mostly affected by the weakly bound effects in the nuclei being studied, while the contribution of charge symmetry breaking is small as discussed before. The reduction factors depend on the single particle energies of $1s_{1/2}$ orbit. From ^{17}F to other nuclei, the Hamiltonians need to be changed because of the different bindings of $1s_{1/2}$ orbit. As some nuclei being studied have no or insufficient experimental information to obtain the single particle energy of $1s_{1/2}$ orbit, we do not include this nucleus-dependent effect in present work. The $1s_{1/2}$ orbits in some nuclei are beyond the proton decay threshold. Such as, the first $1/2^+$ state of ^{19}Na, almost a purely single $1s_{1/2}$ state, is 1.067 MeV beyond the proton threshold. More specific studies including nucleus-dependent and continuum effect may be helpful in order to understand the structure of these nuclei.

Figure 5 shows the comparisons between data and calculations with USD and USD* for the $A = 21$ mirror pair, resulting in a $5/2^+$ ground state for ^{21}Al, which supports the experimental assignment. An $1/2^+$ state is predicted. The MED is not large enough to reverse the $5/2^+$ and $1/2^+$ states. The one-proton separation energy in $5/2^+$ and $1/2^+$ states of ^{21}Al are -1.27 and -2.02 MeV in calculations with the USD* interaction.

The ground-state spin of the nucleus ^{22}Al has not yet been determined experimentally. For its mirror nucleus ^{22}F, the ground state is assigned to be a 4^+ state [8]. Meanwhile a low-lying 3^+ state has also been observed at 71.6 keV. The shell-model calculations can reasonably reproduce these states. Our calculations suggest that these two states are dominated by the coupling $|0d^1_{5/2,t} \otimes 0d^{-1}_{5/2,t'}\rangle$ where $t = n$, $t' = p$ (or vice versa) denoting the isospin of the orbits. For the 3^+ state the

TABLE III. Calculated reduction factors for the six proton-neutron TBME in which the proton $1s_{1/2}$ orbit is involved.

TBME ($\langle ij\|V\|kl\rangle^{pn}_{JT}$)	Reduction factor
$\langle 1s_{1/2}0d_{5/2}\|V\|1s_{1/2}0d_{5/2}\rangle^{pn}_{31}$	0.78
$\langle 1s_{1/2}0d_{5/2}\|V\|1s_{1/2}0d_{5/2}\rangle^{pn}_{21}$	0.84
$\langle 1s_{1/2}0d_{5/2}\|V\|(0d_{5/2})^2\rangle^{pn}_{21}$	0.87
$\langle 1s_{1/2}0d_{5/2}\|V\|1s_{1/2}0d_{5/2}\rangle^{pn}_{30}$	0.81
$\langle 1s_{1/2}0d_{5/2}\|V\|1s_{1/2}0d_{5/2}\rangle^{pn}_{20}$	0.80
$\langle 1s_{1/2}0d_{5/2}\|V\|(0d_{5/2})^2\rangle^{pn}_{30}$	0.87

TABLE IV. Experimental and calculated binding and excitation energies (in MeV) of $^{22-24}$Al and ^{23,24}Si with the original and modified USD Hamiltonians. The last column gives the experimental excitation energies of the corresponding states in their mirror nuclei. Data are from Ref. [8, 35, 37, 38].

$spin^{parity}$	Expt.	USD*	USD*($V^{pn}_{T=1}$)	USD*($V^{pn}_{T=1,0}$)	USD	Expt.(mirror nuclei)
	^{22}Al					^{22}F
4^+		149.69	149.68	149.60	149.71	149.74[a]
3^+		0.14	0.15	0.18	0.19	0.07
2^+		0.64	0.68	0.76	0.71	0.71
	^{23}Al					^{23}Ne
$5/2^+$	168.72	168.90	168.88	168.68	168.88	168.94[a]
$1/2^+$	0.55	0.59	0.57	0.79	1.00	1.02
$3/2^+$	1.62	1.56	1.56	1.72	1.77	1.70
$7/2^+$	1.77	1.70	1.70	1.76	1.76	1.82
	^{24}Al					^{24}Na
4^+	183.59	183.72	183.71	183.40	183.68	183.77[a]
1^+	0.43	0.43	0.43	0.50	0.45	0.47
2^+	0.51	0.53	0.54	0.63	0.59	0.56
1^+	1.09	0.87	0.87	1.06	1.09	1.35
	^{23}Si					^{24}F
$5/2^+$		151.95	151.94	151.79	151.99	151.99[a]
	^{24}Si					^{24}Ne
0^+	172.02	172.48	172.46	172.17	172.50	172.51[a]
2^+	1.88	2.04	2.04	2.13	2.15	1.98
2^+	3.44	3.49	3.46	3.58	3.74	3.87

[a] The energy listed here has been modified to be comparable with the binding energy of its mirror partner through $E = BE(A,Z)_{expt.} + E_C(Z) - E_C(Z')$ where $E_C(Z)$ is the Coulomb correction energy and Z' is the proton number of its mirror partner.

TABLE V. Comparison of experimental and calculated $B(GT^+)/B(GT^-)$ values, where $B(GT^+)$ and $B(GT^-)$ are the Gamow-Teller strengths for the β^+ and β^- decays from ^{24}Si and ^{24}Ne, respectively. The calculated results are obtained with the original (for ^{24}Ne) and modified (for ^{24}Si) USD, USDA and USDB Hamiltonians. Experimental values are taken from Ref. [37].

		$\langle p, s_{1/2} \vert n, s_{1/2}\rangle = 1.0$			$\langle p, s_{1/2} \vert n, s_{1/2}\rangle = 0.9$		
	Expt.	USD	USDA	USDB	USD	USDA	USDB
$B(GT^+, 1^+_1)/B(GT^-, 1^+_1)$	0.78(11)	0.96	0.90	0.98	0.85	0.73	0.85
$B(GT^+, 1^+_2)/B(GT^-, 1^+_2)$	0.90(8)	0.88	0.93	0.85	0.84	0.87	0.82

second largest component is $|1s^1_{1/2,t} \otimes 0d^{-1}_{5/2,t'}\rangle$ which may induce a large MED. Indeed, the MED of the 3^+ state between ^{22}F and ^{22}Al are as large as 57, 69 and 67 keV in calculations with the USD, USDA and USDB interactions, respectively. From these results, the 3^+ state in ^{22}Al is predicted to be above the 4^+ state, which is calculated to be the ground state in the present work, by less than 15 keV. An analysis through the β decay of ^{22}Al also suggests that the ground state of ^{22}Al is most likely to be the 4^+ state [31].

The modified shell-model Hamiltonians can also give a good description to the binding energies of the $N = 8$ isotones, ^{18}Ne, ^{19}Na and ^{20}Mg, as shown in Table II. In these cases only the proton-proton part of the two-body interaction, V^{pp}, contributes to the binding and excitation energies. The binding energy is calculated as [14],

$$BE(A,Z) = BE(A,Z)^r + BE(^{16}\mathrm{O}) - E_C(Z), \quad (1)$$

where $BE(A,Z)^r$ and $BE(^{16}\mathrm{O})$ denote the shell-model energy of the nucleus (A,Z) relative to the ^{16}O core and the experimental binding energy of the ^{16}O core, respectively. $E_C(Z)$ is the Coulomb correction energy, which is 7.45 ($Z = 10$), 11.73 ($Z = 11$), 16.47 ($Z = 12$), 21.48 ($Z = 13$) and 26.78 ($Z = 14$) MeV [14]. For the nuclei investigated, the USD interaction gives on average 0.1 MeV better results for the binding energies in comparison with those of USDA and USDB in both proton- and neutron-rich side. This may be due to the fact that the USDA and USDB interactions are built in a broader basis by including the binding energies of many extreme neutron-rich nuclei including ^{24}O in the fitting besides

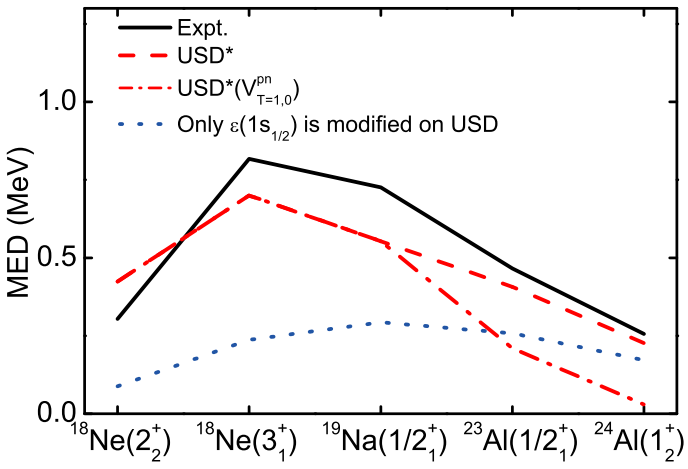

FIG. 9. (Color online) Experimental and calculated MED for selected states in which the experimental values are larger than 200 keV.

the nuclei of concern.

For nuclei $^{22-24}$Al and $^{23-24}$Si, one needs to consider the reduction effect of the interaction matrix element of V^{pn}, which also contribute to the binding and excitation energies of those nuclei, that are related to the weakly bound proton $1s_{1/2}$ orbit. Table III presents the related reduction factors V^{pn}/V^{np} which are evaluated by the same method to obtain V^{pp}/V^{nn}.

We modified on USD* with V^{pn}/V^{np} in two steps. Firstly, only $T = 1$ channel of the V^{pn}/V^{np} is modified, labeled as USD*($V^{pn}_{T=1}$). Secondly, both the $T = 1$ and $T = 0$ channel of V^{pn}/V^{np} are modified on USD*, labeled as USD*($V^{pn}_{T=1,0}$). Our calculations for nuclei $^{22-24}$Al and ^{23,24}Si are given in Table IV together with experimental data. For comparison, in the last column of the table we also give the experimental excitation energies of the corresponding states of the mirror partners of the nuclei of concern. It should be mentioned that the USD interaction, where isospin symmetry is assumed, will give the same results for the mirror partner.

Table IV shows that the $T = 1$ channel contribute little to both binding and excitation energies compared with USD* (on average 14 keV difference for these states). On the other hand, the modification of the strongly attractive $T = 0$ channel changes significantly both binding and excitation energies compared with USD* (on average 150 keV difference for these states). As indicated in Ref. [36], the monopole channel of the $T = 0$ central force, which is strongly attractive, contributes a lot to the binding energies in *sd* shell nuclei, while the contributions of two components in $T = 1$ channel of the central force are canceled to a large extent.

As shown in Table IV, the modification of $T = 0$ channel well reproduces the binding energy difference between the proton-rich nuclei and their mirror partners. Regarding excitation energies (and their MED's), the comparison to experimental data shows varying agreement. For the pair ^{23}Al-^{23}Ne, USD*(V^{pn}) gives comparable results to those by USD*. Regarding the pair ^{24}Al-^{24}Na, we mention that the USD cannot reproduce well the excitation energy of the second 1^+ state of ^{24}Na. The other states also show certain discrepancies, though to less extents. The binding energy is better reproduced by USD*($V^{pn}_{T=1,0}$) considering the original discrepancy between USD result and the observed value in ^{24}Na. For the pair ^{24}Si-^{24}Ne, the overall description is improved by the present method.

In Fig. 9 we compare the experimental and calculated MED's of certain states in which the experimental values are larger than 200 keV. It is seen that shell-model calculations with only the shift of single particle energies taken into account are not enough to describe the experimental MED's, while the USD* including the modification of residual interactions can reproduce the observations. From Table IV and Fig. 9, one can find that the modification of $T = 0$ channel generally gives smaller MED's compared with observed values. This is possibly due to the renormalization effect caused by the modification of $T = 0$ channel which is not included in present study.

For heavier proton-neutron open-shell nuclei such as ^{23,24}Al and ^{24}Si, additional effects may need to be considered in future studies to give a more detailed description. One effect may be the evolution of the single particle energies of $1s_{1/2}$ orbit which are due to nuclear forces but not fully included in USD.

The effect discussed so far also influences the decay properties. For example, the $B(GT)$ value of the β^+ decay from ^{24}Si into ^{24}Al is smaller than that of the decay of the mirror nucleus [37]. In Table V, we present the comparison of $B(GT)$ values between the mirror nuclei, ^{24}Si and ^{24}Ne. The modified USD family can describe the smaller $B(GT)$ values of ^{24}Si compared with those of ^{24}Ne.

The consideration of the weakly bound effect can reduce the $B(GT^+)/B(GT^-)$ value because the overlap between the radial wave functions of the weakly bound proton and well bound neutron $1s_{1/2}$ orbit, $\langle p, s_{1/2}|n, s_{1/2}\rangle$, is smaller than the unity which is assumed in the conventional shell-model calculations. As in Sec. II, we estimate the radial wave function of the proton $1s_{1/2}$ state by using the Woods-Saxon potential. The depth of the potential is taken to be $V_0 = 46.5$ MeV, while other parameters are the same as before. The $1s_{1/2}$ orbital in ^{24}Si is calculated to be weakly bound by 0.1 MeV, which is reasonable by taking into account the fact that both the ground state of ^{25}P and the $1/2^+_1$ state of ^{23}Al are unbound [8]. The radial wave function of the neutron $1s_{1/2}$ state is calculated with harmonic oscillator potential with $A = 24$. The overlap between the calculated proton and neutron radial wave functions is estimated to be $\langle p, s_{1/2}|n, s_{1/2}\rangle = 0.9$. With this value for $B(GT^+)$, Table V suggests that the $B(GT^+)/B(GT^-)$ values obtained with the present reduction factors become sufficiently small giving agreement with the corresponding

experimental data within errors.

IV. SUMMARY

In this paper, the structure of loosely bound proton-rich nuclei around $A = 20$ are investigated within the shell model approach. We start with several well-defined empirical shell-model Hamiltonians constructed for this region. When applying these Hamiltonians to nuclei in the proton-rich side, many of which would be weakly bound, one needs to consider two important points: the shift of single-particle energies and the reduction of the TBME. The reduction factors of TBME are evaluated from the newly introduced NN interaction V_{MU}. The large experimental MED's in ^{18}Ne, ^{19}Na and ^{23}Al are reproduced well by the modified shell-model Hamiltonians. We predict that the 3^+ state in ^{22}Al has an energy slightly higher than the 4^+ ground state. The ground state of ^{21}Al is predicted to be $5/2^+$ state, where the MED is not large enough to make the $1/2^+$ state lower than the $5/2^+$ state.

We have also investigated the Gamow-Teller transitions for the pair of mirror nuclei, ^{24}Si and ^{24}Ne. The observed $B(GT^+)/B(GT^-)$ can be reproduced well by taking into account the weakly bound nature of the proton $1s_{1/2}$ orbit.

ACKNOWLEDGEMENT

This work has been supported by the National Key Basic Research Program of China under Grant No. 2013CB834400, the National Natural Science Foundation of China Under Grant Nos. 11305272, 11235001, 11320101004, the Specialized Research Fund for the Doctoral Program of Higher Education Under Grant No. 20130171120014, and by Japanese MEXT Grant-in-Aid for Scientific Research (A) 20244022. C.Q. acknowledges the supports by the Swedish Research Council (VR) under grant Nos. 621-2010-4723 and 621-2012-3805, and the computational support provided by the Swedish National Infrastructure for Computing (SNIC) at PDC and NSC.

[1] H. Grawe, K. Langanke, and G. Martínez-Pinedo, Rep. Prog. Phys. **70**, 1525 (2007).
[2] D. W. Bardayan *et al.*, Phys. Rev. Lett. **83**, 45 (1999); D. W. Bardayan *et al.*, Phys. Rev. C **62**, 055804 (2000).
[3] A. Bohr, B. R. Mottelson, *Nuclear Structure* (Benjamin, New York, 1969), vol. 1.
[4] B. A. Brown, Prog. Part. Nucl. Phys. **47**, 517 (2001).
[5] D. D. Warner, M. A. Bentley, and P. Van Isacker, Nat. Phys. **2**, 311 (2006).
[6] M. A. Bentley and S.M. Lenzi, Prog. Part. Nucl. Phys. **59**, 497 (2007).
[7] C. Qi and F. R. Xu, Nucl. Phys. **A814**, 48 (2008).
[8] http://www.nndc.bnl.gov/nudat2/
[9] R. G. Thomas, Phys Rev. C **88**, 1109 (1952).
[10] J. B. Ehrman, Phys Rev. C **81**, 412 (1951).
[11] W. E. Ormand and B. A. Brown, Nucl. Phys. **A491**, 1 (1989).
[12] K. Ogawa, H. Nakada, S. Hino, and R. Motegi, Phys. Lett. **B464**, 157 (1999).
[13] B. H. Wildenthal, Prog. Part. Nucl. Phys. **11**, 5 (1984); B. A. Brown and B. H. Wildenthal, Annu. Rev. Nucl. Part. Sci. **38**, 29 (1988).
[14] B. A. Brown and W. A. Richter, Phys. Rev. C **74**, 034315 (2006).
[15] T. Otsuka, T. Suzuki, M. Honma, Y. Utsuno, N. Tsunoda, K. Tsukiyama, and M. Hjorth-Jensen, Phys. Rev. Lett. **104**, 012501 (2010).
[16] T. T. S. Kuo, F. Krmpotić, and Y. Tzeng, Phys. Rev. Lett. **78**, 2708 (1997)
[17] K. Heyde, Basic Ideas and Concepts in Nuclear Physics, 2nd ed. (IOP, Bristol, 1999).
[18] R. Morlock *et al.*, Phys. Rev. Lett. **79**, 3837 (1997).
[19] Z. Ren, A. Faessler, and A. Bobyk, Phys. Rev. C **57**, 2752 (1998).
[20] T. Vertse, K.F. Pál, and Z. Balogh, Comput. Phys. Commun. **27**, 309 (1982).
[21] R. Machleidt, Phys. Rev. C **63**, 024001 (2001).
[22] G. Bertsch, J. Borysowicz, H. McManus, and W. G. Love, Nucl. Phys. **A284**, 399 (1977).
[23] C.X. Yuan, T. Suzuki, T. Otsuka, F.R. Xu, and N. Tsunoda, Phys Rev. C **85**, 064324 (2012).
[24] Y. Utsuno, T. Otsuka, B. A. Brown, M. Honma, T. Mizusaki, and N. Shimizu, Phys Rev. C **86**, 051301(R) (2012).
[25] T. Suzuki and M. Honma, Phys Rev. C **87**, 014607 (2013).
[26] A. Signoracci, B. A. Brown, and M. Hjorth-Jensen, Phys. Rev. C **83**, 024315 (2011).
[27] http://www.nscl.msu.edu/∼brown/resources/resources.html
[28] H. T. Fortune and R. Sherr, Phys. Rev. C **87**, 044315 (2013).
[29] H. T. Fortune and R. Sherr, Phys. Rev. C **83**, 057301 (2011).
[30] H. T. Fortune and R. Sherr, Phys. Rev. C **87**, 014316 (2013).
[31] N. L. Achouri *et al.*, Eur. Phys. J. A **27**, 287 (2006)
[32] C. Angulo *et al.*, Phys. Rev. C **67**, 014308 (2003).
[33] M.G. Pellegriti *et al.*, Phys. Lett. **B659**, 864 (2008).
[34] A. Gade *et al.*, Phys. Rev. C **76**, 024317 (2007).
[35] A. Gade *et al.*, Phys. Lett. **B666**, 218 (2008).
[36] A. Umeya, S. Nagai, G. Kaneko, and K. Muto Phys. Rev. C **77**, 034318 (2008).
[37] Y. Ichikawa *et al.*, Phys. Rev. C **80**, 044302 (2009).
[38] M. Wang, G. Audi, A. H. Wapstra, F. G. Kondev, M. MacCormick, X. Xu, and B. Pfeiffer, Chin. Phys. C 36(12) (2012) 1603.